The 11th International Conference on Ubiquitous Robots and Ambient Intelligence (URAI 2014)
Nov. 12 – 15, 2014 at Double Tree Hotel by Hilton, Kuala Lumpur, Malaysia

Learning Motion and Impedance Behaviors from Human Demonstrations

Matteo Saveriano[1] and Dongheui Lee[1]

[1]Chair of Automatic Control Engineering, Technical University of Munich, Munich, Germany
(Tel : +49-89-289-268840, +49-89-289-25780; E-mail: matteo.saveriano@tum.de, dhlee@tum.de)

Abstract - Human-robot skill transfer has been deeply investigated from a kinematic point of view, generating various approaches to increase the robot knowledge in a simple and compact way. Nevertheless, social robotics applications require a close and active interaction with humans in a safe and natural manner. Torque controlled robots, with their variable impedance capabilities, seem a viable option toward a safe and profitable human-robot interaction. In this paper, an approach is proposed to simultaneously learn motion and impedance behaviors from tasks demonstrations. Kinematic aspects of the task are represented in a statistical way, while the variability along the demonstrations is used to define a variable impedance behavior. The effectiveness of our approach is validated with simulations on real and synthetic data.

Keywords - Learning from Demonstrations, variable impedance control, state-dependent behavior.

1. Introduction

In real applications, the robot is required to execute complex tasks and to adapt its behavior to guarantee a safe interaction with humans and dynamic environments. Skills acquisition and their compact representation as motion primitives, as well as on-line adaptation of those skills to new scenarios [1], are of importance both in industrial and service contexts.

Leaning from Demonstration (LfD) is a powerful tool to teach skills in a simple and natural way. In LfD an expert user provides some demonstrations of a task, physically guiding the robot or executing the task himself. Hence, also users that are not familiar with robot programming can easily teach new skills. Among the others, approaches have been developed to learn stable dynamical systems (DS) from demonstration [2, 3]. DS driven robots are guaranteed to reach the desired position and can react in real-time to external perturbations, such as changes in the goal position or unforeseen obstacles [4-8].

Nevertheless, in dynamic and highly populated environments, sudden perturbations are expected and a stiff controller will generate high forces, making the interaction dangerous. Impedance control [9] is a suitable approach to control the dynamic response of the robot. The goal of impedance control is to regulate the mechanical impedance of the manipulator, i.e. making the robot end-effector acting as a mass-spring-damping system. Changing the impedance parameters during the task execution will generate richer behaviors. Hence, the new problem arises of how a robot can learn impedance behaviors.

Impedance in humans has been studied to understand the roles of the different body parts, such as muscles, tendons, brain and spinal cord, in modulating impedance during the interactions with the environment. A device capable to measure human stiffness is used in [10] for examining the so-called equilibrium-point control hypothesis during multijoint arm movements. In [11] a similar setup is adopted to show that humans learn an optimal variable impedance to stabilize intrinsically unstable movements. Bio-inspired algorithms have also been developed to mimic human impedance with robots [12].

The significant differences in kinematics and dynamics make hard for robots to reproduce humans impedance. Alternative solutions have been developed in the LfD framework. The main idea is to learn the stiffness from the variability of human demonstrations, i.e. setting high stiffness values (accurate tracking) where the demonstrations are similar and low values (compliance) where the demonstrations exhibit high variability. Obviously, it is implicitly assumed that the user demonstrates the task with high variability where he wants the robot to be compliant and low variability where the robot must be stiff.

This idea is applied in [13] to learn the time-varying proportional gains (stiffness) of a mixture of K proportional-derivative systems used to represent the desired acceleration trajectory. The time-dependent stiffness is inversely proportional to the variance along the demonstrations. In [14] collaborative impedance robot behaviors are learned. The core idea is to virtually connect the robot's end-effector to a set of virtual springs driving the robot behavior. The time-varying stiffness matrices are learned using a weighted least square approach. Finally, in [15] a technique to modify robot's stiffness online is presented. The robot executes a task with high, constant stiffness in each time instant and the user can only decrease the stiffness by shaking the robot.

The result of the previous approaches is a time-varying stiffness. For many tasks, a state-varying, time-independent impedance behavior is desirable, being more robust to delays in the execution of the task. Indeed, a time-varying stiffness can fail to provide adequate impedance behaviors at the right time and in the right place when the execution time changes. Our approach consists in learning a state-dependent stiffness exploring the variability of human demonstrations. Firstly, the kinematic aspects (position and velocity) of the task are encoded in a time-invariant DS as in [2]. Secondly, the variability of the demonstrations, captured by Gaussian mixture models [16], generates a continuous, state-dependent stiffness matrix. A Cartesian force is then computed that drives the robot to complete the task.

The rest of the paper is organized as follows. Section

2 describes the adopted control strategy and the proposed impedance learning algorithm. In Sec. 3 we present the simulation results. Section 4 states the conclusions and the future works.

2. Proposed Approach

In this section we present our approach for learning state-dependent motion and impedance behaviors from human demonstration. Firstly, we underline some important concepts concerning the SEDS algorithm [2], used to train a motion primitive in the form of a globally asymptotically stable (GAS) DS. Secondly, we explain how the stiffness is estimated from Gaussian regression. Finally, we discuss the control law used to execute the desired behavior.

2.1 Learning stable motion primitives

We assume that the set of N demonstrations $\{\boldsymbol{x}^{t,n}, \dot{\boldsymbol{x}}^{t,n}\}_{t=0,n=1}^{T,N}$, where $\boldsymbol{x} \in \mathbb{R}^d$ is the position and $\dot{\boldsymbol{x}} \in \mathbb{R}^d$ the velocity, are instances of a first order, nonlinear DS in the form:

$$\dot{\boldsymbol{x}} = \boldsymbol{f}(\boldsymbol{x}) + \boldsymbol{\eta} \,, \tag{1}$$

where $\boldsymbol{f}(\boldsymbol{x}) : \mathbb{R}^d \rightarrow \mathbb{R}^d$ is a nonlinear continuous function with a unique equilibrium point in $\dot{\boldsymbol{x}}^* = \boldsymbol{f}(\boldsymbol{x}^*) = \boldsymbol{0}$, and $\boldsymbol{\eta} \in \mathbb{R}^d$ is a zero mean Gaussian noise. Having the noise distribution a zero mean it is possible to use regression to estimate the noise-free model $\dot{\boldsymbol{x}} = \hat{\boldsymbol{f}}(\boldsymbol{x})$.

To estimate the noise-free DS, a probabilistic framework is used that models $\hat{\boldsymbol{f}}$ as a finite mixture of Gaussian functions. Therefore, the nonlinear function $\hat{\boldsymbol{f}}$ is parametrized by the priors $\mathcal{P}(k) = \pi^k$, the means $\boldsymbol{\mu}^k$ and the covariance matrices $\boldsymbol{\Sigma}^k$ of the $k = 1, \ldots, K$ Gaussian functions. The means and covariance matrices are defined by:

$$\boldsymbol{\mu}^k = \begin{bmatrix} \boldsymbol{\mu}_x^k \\ \boldsymbol{\mu}_{\dot{x}}^k \end{bmatrix}, \quad \boldsymbol{\Sigma}^k = \begin{bmatrix} \boldsymbol{\Sigma}_x^k & \boldsymbol{\Sigma}_{x\dot{x}}^k \\ \boldsymbol{\Sigma}_{\dot{x}x}^k & \boldsymbol{\Sigma}_{\dot{x}}^k \end{bmatrix}. \tag{2}$$

A probability density function $\mathcal{P}(\boldsymbol{x}^{t,n}, \dot{\boldsymbol{x}}^{t,n}; \boldsymbol{\Theta})$, in the form of a mixture of Gaussian components, is associated to each point in the demonstrated trajectories:

$$\mathcal{P}(\boldsymbol{x}^{t,n}, \dot{\boldsymbol{x}}^{t,n}|\boldsymbol{\Theta}) = \sum_{k=1}^{K} \pi^k \mathcal{N}(\boldsymbol{x}^{t,n}, \dot{\boldsymbol{x}}^{t,n}|\boldsymbol{\mu}^k, \boldsymbol{\Sigma}^k) \,, \tag{3}$$

where $\boldsymbol{\Theta} = \{\pi^1, \boldsymbol{\mu}^1, \boldsymbol{\Sigma}^1, \ldots, \pi^K, \boldsymbol{\mu}^K, \boldsymbol{\Sigma}^K\}$ are the prior, the mean and the covariance matrix of each component. Taking the posterior mean probability $\mathcal{P}(\dot{\boldsymbol{x}}|\boldsymbol{x})$ as an estimation of $\hat{\boldsymbol{f}}$ yields [16]:

$$\dot{\boldsymbol{x}} = \hat{\boldsymbol{f}}(\boldsymbol{x}) = \sum_{k=1}^{K} h^k(\boldsymbol{x})(\boldsymbol{A}^k\boldsymbol{x} + \boldsymbol{b}^k) \,, \tag{4}$$

where:

$$\begin{aligned} \boldsymbol{A}^k &= \boldsymbol{\Sigma}_{\dot{x}x}^k (\boldsymbol{\Sigma}_x^k)^{-1} \\ \boldsymbol{b}^k &= \boldsymbol{\mu}_{\dot{x}}^k - \boldsymbol{A}^k \boldsymbol{\mu}_x^k \\ h^k(\boldsymbol{x}) &= \frac{\pi^k \mathcal{N}(\boldsymbol{x}|\boldsymbol{\mu}_x^k, \boldsymbol{\Sigma}_x^k)}{\sum_{i=1}^{K} \pi^i \mathcal{N}(\boldsymbol{x}|\boldsymbol{\mu}_x^i, \boldsymbol{\Sigma}_x^i)} \,. \end{aligned} \tag{5}$$

The nonlinear function $\hat{\boldsymbol{f}}$ is then expressed as a nonlinear sum of linear dynamical systems. To guarantee that the DS in Eq. (4) has a GAS equilibrium in $\boldsymbol{x}^*$, the parameters $\boldsymbol{\Theta}$ can be estimated solving the following optimization problem [2]:

$$\min_{\boldsymbol{\Theta}} J(\boldsymbol{\Theta}) = -\sum_{n=1}^{N}\sum_{t=0}^{T} \log \mathcal{P}(\boldsymbol{x}^{t,n}, \dot{\boldsymbol{x}}^{t,n}|\boldsymbol{\Theta})$$

subject to

$$\left.\begin{aligned} &\boldsymbol{b}^k = -\boldsymbol{A}^k\boldsymbol{x}^* \\ &\boldsymbol{A}^k \text{ negative definite} \\ &\boldsymbol{\Sigma}^k \text{ positive definite} \\ &0 \leq \pi^k \leq 1 \\ &\sum_{k=1}^{K} \pi^k = 1 \end{aligned}\right\} \quad \forall k \in 1, \ldots, K \tag{6}$$

where $\mathcal{P}(\boldsymbol{x}^{t,n}, \dot{\boldsymbol{x}}^{t,n}|\boldsymbol{\Theta})$ is defined in Eq. (3).

2.2 Learning variable stiffness

The probabilistic framework described in Sec. 2.1 can be also used to retrieve an estimation of the stiffness for each position, following the principle that the robot must be stiff where demonstrations are similar and compliant otherwise. The variability of the demonstrations, at the position level[1], is captured by the mixture regression in the covariance matrices $\boldsymbol{\Sigma}_x^k$ (Eq. (2)). Given the current robot position $\boldsymbol{x}$ we calculate the covariance matrix:

$$\hat{\boldsymbol{\Sigma}}_x = \sum_{k=1}^{K} (h^k(\boldsymbol{x}))^2 \boldsymbol{\Sigma}_x^k \,, \tag{7}$$

where $h^k(\boldsymbol{x})$ is defined in Eq. (5). In practise, we weight the contribution of each matrix using the responsibility $h^k(\boldsymbol{x})$ that each Gaussian has in $\boldsymbol{x}$. The computed covariance matrix is symmetric and positive definite. Hence, we are allowed to calculate its eigenvalues decomposition:

$$\hat{\boldsymbol{\Sigma}}_x = \boldsymbol{E}\boldsymbol{\Lambda}\boldsymbol{E}^{-1} \,, \tag{8}$$

where $\boldsymbol{E}$ is the matrix of the eigenvectors (principal directions) and $\boldsymbol{\Lambda} = \mathrm{diag}(\lambda^1, \ldots, \lambda^d)$ is the diagonal matrix of the eigenvalues.

The root square of the eigenvalues of $\hat{\boldsymbol{\Sigma}}_x$, $\sigma^i = \sqrt{\lambda^i}$, represents the variability (standard deviation) of the data along each direction. We propose to construct the stiffness saving the principal directions of $\hat{\boldsymbol{\Sigma}}_x$, choosing the eigenvalues inversely proportional to σ^i. The stiffness matrix can be written as:

$$\boldsymbol{K} = \boldsymbol{E}\boldsymbol{S}\boldsymbol{E}^{-1} \,, \tag{9}$$

[1] The variability at the velocity level, or between position and velocity is not taken into account. We claim, in fact, that the user can hardly take into account these kinds of variability while he performs the demonstrations.

where $\boldsymbol{S} = \text{diag}(s^1, \ldots, s^d)$. Between the eigenvalues s^i of the stiffness matrix and σ^i the following nonlinear inverse relationship holds:

$$s^i(\sigma^i) = \begin{cases} s_{min} & \sigma^i > \sigma_{max} \\ p_1 \left(1 - \tanh\left(p_2\right)\right) + s_{min} & \sigma_{min} \leq \sigma^i \leq \sigma_{max} \\ s_{max} & \sigma^i < \sigma_{min} \end{cases} \tag{10}$$

where

$$p_1 = \frac{s_{max} - s_{min}}{2}, \; p_2 = \frac{2k_0}{s_{max}} \left(\sigma^i - \frac{\sigma_{max} - \sigma_{min}}{2} \right) . \tag{11}$$

The stiffness values in each direction are bounded by the tunable parameters s_{min} and s_{max}. The parameters σ_{min}, σ_{min} and k_0 are also tunable parameters for the learning system. The nonlinear relationship in Eq. (10), (11) is shown in Fig. 1. There are two saturation areas corresponding to $\sigma^i > \sigma_{max}$ and $\sigma^i < \sigma_{min}$ where the eigenvalues assume the values s_{min} and s_{max} respectively. Among them there is an almost linear area in which s^i is inversely proportional to σ^i. The size of the saturation areas and, consequently, the slope of the linear part can be modulated by varying k_0. To avoid rapid changes in the stiffness values, the adopted function guarantees a smooth transition between the linear area and the saturation ones.

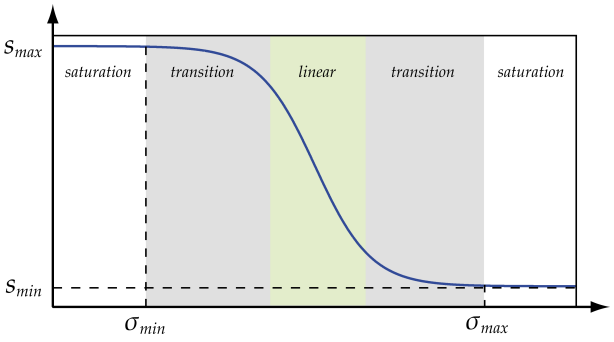

Fig. 1 Nonlinear relationship between covariance and stiffness matrices eigenvalues.

2.3 Control law

We assume that our robot can be controlled by an impedance control law (torque feedback) [9]. Given the desired velocity, position and stiffness, the following control law realizes the desired motion-impedance behavior:

$$\boldsymbol{\tau} = \boldsymbol{J}^{\mathrm{T}} \boldsymbol{F} + \boldsymbol{n}(\boldsymbol{q}, \dot{\boldsymbol{q}}, \ddot{\boldsymbol{q}}) \, , \tag{12}$$

where $\boldsymbol{\tau}$ is the input torque, $\boldsymbol{J}$ is the Jacobian of the manipulator and $\boldsymbol{n}(\boldsymbol{q}, \dot{\boldsymbol{q}}, \ddot{\boldsymbol{q}})$ compensates the nonlinearities in the dynamical model of the robot.

The force term $\boldsymbol{F}$ is chosen as:

$$\boldsymbol{F} = \boldsymbol{K}\boldsymbol{x} + \boldsymbol{D}\dot{\boldsymbol{x}} \, , \tag{13}$$

where $\boldsymbol{K}$ is the state-dependent stiffness matrix in Eq. (9), $\dot{\boldsymbol{x}}$ is the velocity computed in Eq. (4) and $\boldsymbol{x}$ is obtained integrating $\dot{\boldsymbol{x}}$. The damping matrix $\boldsymbol{D}$ is chosen to have the same eigenvectors (principal directions) of the stiffness matrix (Eq. (9)) with eigenvalues $d^i = 2\sqrt{s^i}$, $i = 1, \ldots, d$. Being the DS in Eq. (4) globally asymptotically stable and $\boldsymbol{K}$, $\boldsymbol{D}$ positive definite, the force term drives the robot towards the desired position imposing a state dependent impedance behavior.

3. Simulation Results

In this section we validate the effectiveness of our approach in two cases. The first simulation is used to show how the task constraints are learned from demonstrations. Synthetic 2-dimensional data are used. In the second experiment, a point-to-point task is learned from demonstrations.

3.1 Learning task constraints

In this simulation we generate three 2-dimensional position trajectories[2] that are constrained at the beginning and at the end of the motion. The trajectories start almost identical, exhibit variations and end again identical.

The results obtained learning the DS in Eq. (4) with three Gaussian components are shown in Fig. 2. As expected, the algorithm is able to detect constraints in the demonstrations and to return coherent values in terms of position and stiffness. The covariance matrices $\boldsymbol{\Sigma}_x^k$, $k = 1, \ldots, 3$ are represented as ellipses in Fig. 2(a), where the dimension of each axis of the ellipse is proportional to the standard deviation in that direction. The two covariance matrices close to the constrained areas have a small variance, while the other has a big variance. As a results, the covariance matrix $\hat{\boldsymbol{\Sigma}}_x$, computed by the regression technique in Sec. 2.2, has a small standard deviation for points close to the constrained areas, big otherwise (Fig. 2(b)). Conversely, the learned stiffness is big where the motion is constrained and small otherwise (Fig. 2(c)).

3.2 Point-to-point motion

In this simulation we learn a point-to-point motion task from human demonstrations. The data, collected by kinesthetic teaching[2], are shown in Fig. 3(a). The demonstrations have high variability at the beginning of the motion, while they converge to the goal position at the end.

Again, the learning algorithm is able to capture this variability. The two learned covariance matrices $\boldsymbol{\Sigma}_x^k$, $k = 1, 2$ are represented as ellipsoids in Fig. 3(a), where the dimension of each axis of the ellipsoid is proportional to the standard deviation in that direction. The covariance matrix closer to the initial points in the trajectories has bigger covariance than the other, being the variability at the beginning of the motion considerably bigger. The generated motion, obtained integrating the learned DS velocity with a sample time $\delta t = 0.01s$, is shown in Fig. 3(b). As expected, the trajectory converges to the goal position, being the learned DS globally asymptotically stable. Figure 3(c) shows the eigenvalues of the covariance matrix $\hat{\boldsymbol{\Sigma}}_x$. The eigenvalues have big values at the beginning of the motion (high variability) and decrease while the trajectory converges to the goal position

[2]The velocity is computed by numerical differentiation.

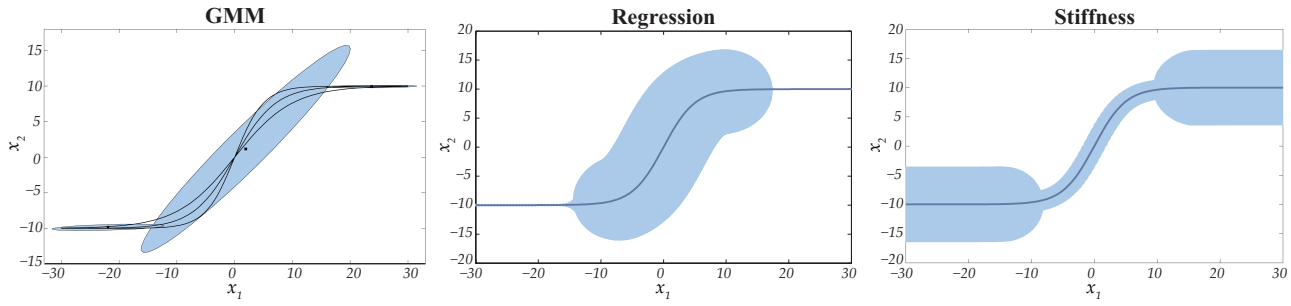

(a) (b) (c)

Fig. 2 Results of the learning algorithm on the synthetic dataset. (a) Demontrations (black lines) and learned model. (b) Smooth motion retrieved using GMR and related covariance matrix $\hat{\mathbf{\Sigma}}_x$. (c) Learned stiffness.

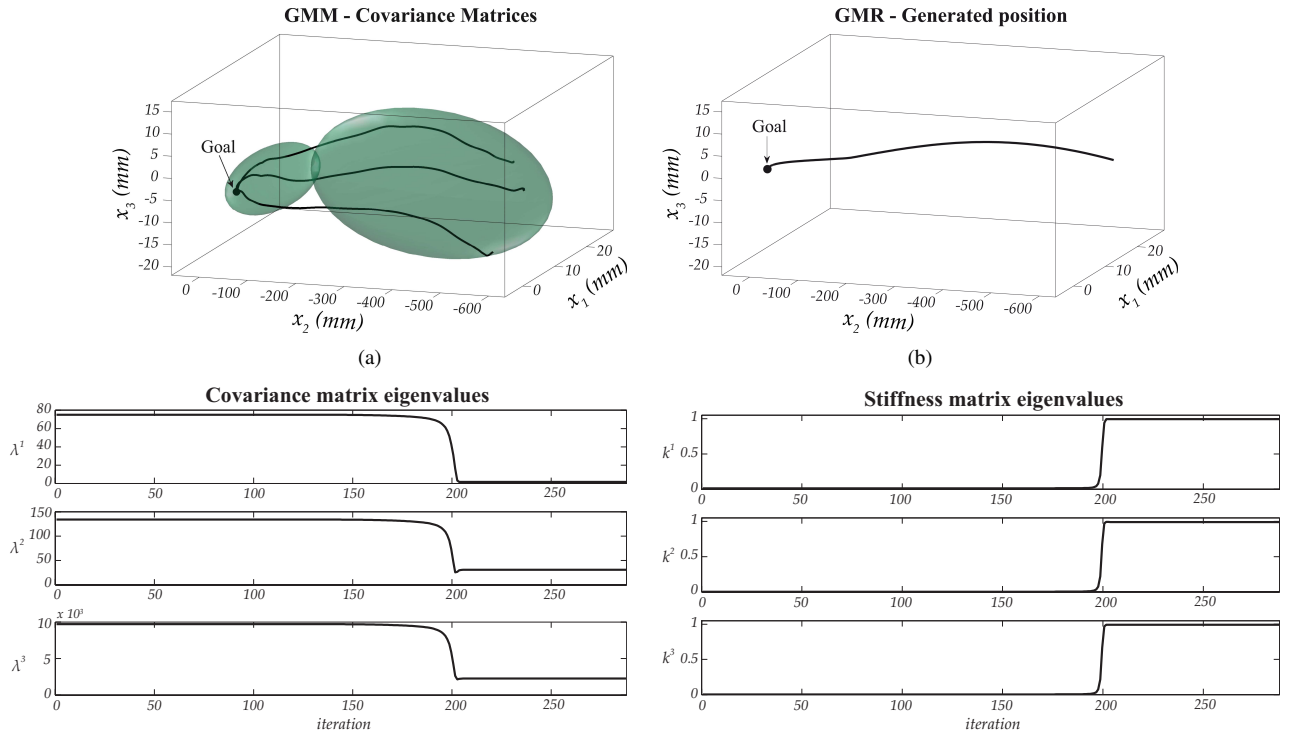

(a) (b) (c) (d)

Fig. 3 Results of the learning algorithm on the point-to-point motion dataset. (a) Demontrations (black lines) and learned model. (b) Smooth motion retrieved using GMR. (c) Eigenvalues of the covariance matrix $\hat{\mathbf{\Sigma}}_x$ for the generated motion. (d) Eigenvalues of the stiffness matrix, normalized to 1.

(low variability). Conversely, the learned stiffness matrix eigenvalues in Fig. 3(d) are small at the beginning of the motion (high variability) and increase while the trajectory converges to the goal position (low variability). The eigenvalues in Fig. 3(d) are obtained firstly scaling the standard deviation along each direction, i.e. the square root σ^i of the eigenvalues of $\hat{\mathbf{\Sigma}}_x$, in the interval $[\sigma_{min} = 1,\ \sigma_{max} = 4]$ and then applying the inverse relationship in Eq. (10) with $[s_{min} = 0,\ s_{max} = 1]$.

The learned DS and stiffness are then used to generate the impedance behavior in Eq. (12)-(13). To this end, we used a dynamic simulator of a KUKA lightweight 7 degree-of-freedom robot [17]. The manipulator end-effector is driven by the learned DS to reach the target position $\boldsymbol{g} = [-0.6\ 0.18\ 0.25]\ m$ (the orientation is kept constant), starting from $\boldsymbol{x}(0) = [-0.56\ -0.42\ 0.22]\ m$. The stiffness eigenvalues range is chosen as $[s_{min} = 50,\ s_{max} = 300]$, while the sample time is chosen as $\delta t = 1ms$. For comparison, the same DS is used to drive the robot with a constant stiffness $K = \mathrm{diag}(300, 300, 300)$.

Firstly, we compare the end-effector position error between the executed trajectory and the generated (integrating the DS) one. As expected, the robot is able to reach the target both with constant and variable stiffness (see Fig. 4). With constant high stiffness, the robot stays significantly closer to the reference trajectory. Hence, as already mentioned, if the goal is an accurate tracking an high stiffness is required.

Secondly, we test the proposed approach when a collision occurs. To simulate a collision, an impulsive external force $f = [20\ 0\ 0]\ N$ is applied for $5ms$ starting

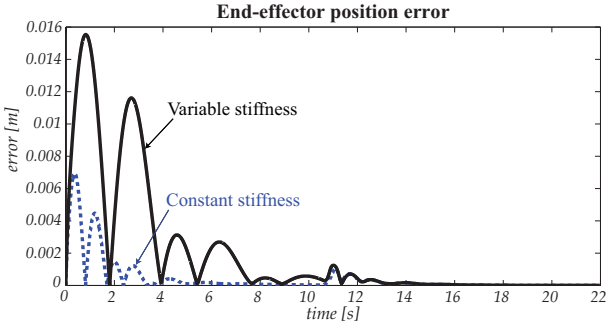

Fig. 4 Norm of the end-effector position error with constant (blue dashed line) and variable (black solid line) stiffness.

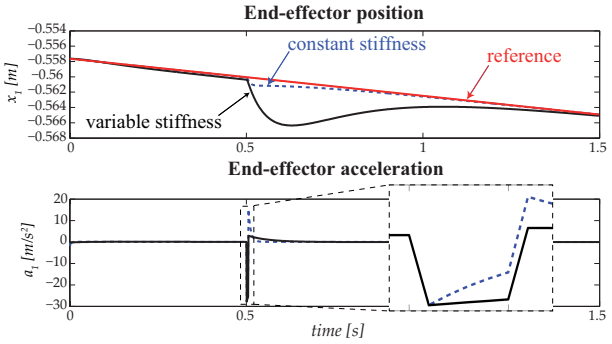

Fig. 5 End-effector position and acceleration when an impulsive force of $20N$ is applied along the x_1 direction. To clearly show the effects of the applied force, only the x_1 axis (the most affected) and the first $1.5s$ of the trajectory are considered.

at $t = 0.5s$. As shown in Fig. 5, when the robot has a small stiffness, the external force generates a big deviation from the reference trajectory. In this case, in fact, the robot accomplish the applied force. Instead, with high stiffness, the robot generates higher accelerations at the end-effector to suddenly react to the external disturbance. This results in a considerably smaller deviation, but into a possibly dangerous behavior. Hence, the learned behavior guarantees a compliant and safe interaction with the environment in a certain area of the state space (until a certain distance from the target). The high stiffness close to the target point guarantees instead to reach and keep the desired final position.

4. Conclusions

We presented an approach to simultaneously learn kinematic and dynamic aspects of a task from human demonstrations. The probabilistic framework offered by Gaussian mixture models was adopted to represent the task in the compact form of an asymptotically stable dynamical system. Hence, the convergence of the motion trajectory to a desired goal position is always guaranteed. The covariance matrices of the mixture components, representing the variability along the demonstrations, were used to retrieve a smooth estimation of a state dependent stiffness matrix. The resulting stiffness is small (compliant behavior) where the demonstrations exhibit high variability, big otherwise. A suitable impedance control law is also presented to realize the desired impedance behavior.

The approach has been currently validated only in simulation and on a simple point-to-point motion task. Our future research will focus on considering more complex tasks, as well as on implementing and testing the proposed solution on real robots.

Acknowledgement

This work has been partially supported by the European Community within the FP7 ICT-287513 SAPHARI project and Technical University of Munich, Institute for Advanced Study, funded by the German Excellence Initiative.

References

[1] D. Lee and C. Ott, "Incremental Kinesthetic Teaching of Motion Primitives Using the Motion Refinement Tube," *Autonomous Robots*, Vol. 31, No. 2, pp. 115-131, 2011.

[2] S. M. Khansari-Zadeh and A. Billard, "Learning Stable Non-Linear Dynamical Systems with Gaussian Mixture Models," *Transaction on Robotics*, Vol. 27, No. 5, pp. 943-957, 2011.

[3] A. Ijspeert, J. Nakanishi, P. Pastor, H. Hoffmann and S. Schaal, "Dynamical Movement Primitives: learning attractor models for motor behaviors," *Neural Computation*, Vol. 25, No. 2, pp. 328-373, 2013.

[4] S. M. Khansari-Zadeh and A. Billard, "A dynamical system approach to realtime obstacle avoidance," *Autonomous Robots*, Vol. 32, No. 4, pp. 433-454, 2012.

[5] M. Saveriano and D. Lee, "Point Cloud based Dynamical System Modulation for Reactive Avoidance of Convex and Concave Obstacles," *Proc. of the IEEE/RSJ International Conference on Intelligent Robots and Systems*, pp. 5380-5387, 2013.

[6] M. Saveriano and D. Lee, "Distance based Dynamical System Modulation for Reactive Avoidance of Moving Obstacles," *Proc. of the IEEE International Conference on Robotics and Automation*, 2014.

[7] S. Haddadin, S. Belder and A. Albu-Schäffer, "Dynamic motion planning for robots in partially unknown environments," *IFAC World Congress*, pp. 6842-6850, 2011.

[8] H. Hoffmann, P. Pastor, D.-H. Park, and S. Schaal, "Biologically-inspired dynamical systems for movement generation: automatic real-time goal adaptation and obstacle avoidance," *Proc. of the IEEE International Conference on Robotics and Automation*, pp. 1534-1539, 2009.

[9] N. Hogan, "Impedance control: An approach to manipulation: Part i, ii, iii," *Journal of Dynamic Sys-*

tems, Measurement, and Control, Vol. 107, No. 1, pp. 1-24, 1985.

[10] H. Gomi and M. Kawato, "Equilibrium-point control hypothesis examined by measured arm stiffness during multijoint movement," *Science* Vol. 272, No. 5258, pp. 117-120, 1996.

[11] E. Burdet, R. Osu, D. W. Franklin, T. E. Milner and M. Kawato, "The central nervous system stabilizes unstable dynamics by learning optimal impedance," *Nature* Vol. 414, No. 6862, pp. 446-449, 2001.

[12] G. Ganesh, A. Albu-Schaffer, M. Haruno, M. Kawato and E. Burdet, "Biomimetic motor behavior for simultaneous adaptation of force, impedance and trajectory in interaction tasks," *Proc. of the IEEE International Conference on Robotics and Automation*, pp. 2705-2711, 2010.

[13] S. Calinon, I. Sardellitti, and D. Caldwell, "Learning-based control strategy for safe human-robot interaction exploiting task and robot redundancies" *Proc. of the IEEE/RSJ International Conference on Intelligent Robots and Systems* pp. 249-254, 2010.

[14] L. Rozo, S. Calinon, D. G. Caldwell, P. Jimenez C. and Torras, "Learning collaborative impedance-based robot behaviors" *Proc. of the AAAI Conference on Artificial Intelligence* pp. 1422-1428, 2013.

[15] K. Kronander and A. Billard, "Online learning of varying stiffness through physical human-robot interaction," *Proc. of the IEEE International Conference on Robotics and Automation*, pp. 1842-1849, 2012.

[16] D. A. Cohn, Z. Ghahramani and M. I. Jordan, "Active Learning with Statistical Models," *Journal of Artificial Intelligence Research*, Vol. 4, No. 1, pp. 129-145, 1996.

[17] R. Bischoff, J. Kurth, G. Schreiber, R. Koeppe, A. Albu-Schaeffer, A. Beyer, O. Eiberger, S. Haddadin, A. Stemmer, G. Grunwald and G. and Hirzinger, "The KUKA-DLR Lightweight Robot arm - a new reference platform for robotics research and manufacturing," *International Symposium on Robotics and German Conference on Robotics*, pp. 1-8, 2010.